Supplement of Clim. Past, 19, 1101–1123, 2023
https://doi.org/10.5194/cp-19-1101-2023-supplement

Climate of the Past
Open Access
EGU

Supplement of

Buoyancy forcing: a key driver of northern North Atlantic sea surface temperature variability across multiple timescales

Bjørg Risebrobakken et al.

Correspondence to: Bjørg Risebrobakken (bjri@norceresearch.no)

The information summarized in Table 2 in the paper is based on information extracted from previously published Pliocene records. To keep consistency and allow for direct comparison when comparing this information to the identified SST anomaly relations, these previously published records were resampled every 100 ka between 5.23 and 3.13 Ma, using a linear integration function in *AnalySeries* (Paillard et al., 1996), and presented as anomalies relative to the mean of their resampled self (100 ka) (as described in Section 2.1 for ODP sites 982, 642 and 907). This approach allows for direct comparison between sites, independent of differences in temporal resolution and absolute age of the raw data points. The anomaly plots based on the resampled datasets were plotted with the purpose to look at global SSTs, AMOC and ventilation of the deep Nordic seas, the Atlantic Equator-to-Pole SST gradient and sea ice/freshwater (Fig. S1-S5). Only datasets that cover the full interval with a resolution that allowed for a 100-ka resampling were included (Table S1). The location of the included sites is shown in Fig. S6.

Figure S1: Northern Hemisphere meridional SST gradient

Figure S2: Ocean circulation

Figure S3: Globally distributed SST records

Figure S4: Meridional SST gradients based on globally distributed SST records

Figure S5: Atmospheric conditions over Norway, based on pollen from Site 642

Figure S6: Map with site locations indicated

Table S1: Overview of sites used

Figure S1. Northern Hemisphere meridional SST gradients using data from sites in Table S1. The upper panel shows data restricted to sites from the Atlantic Ocean and the lower panel show data restricted to sites from the Pacific and Indian Ocean. There is only one site with information from the Indian Ocean (marked with the box). The mid panel show all datapoints used for the upper and lower panel. The different coloured lines and dots represent time intervals where the different SST anomaly relations are identified (specified in the legend underneath). World Ocean Atlas data is from Locarini et al. (2018).

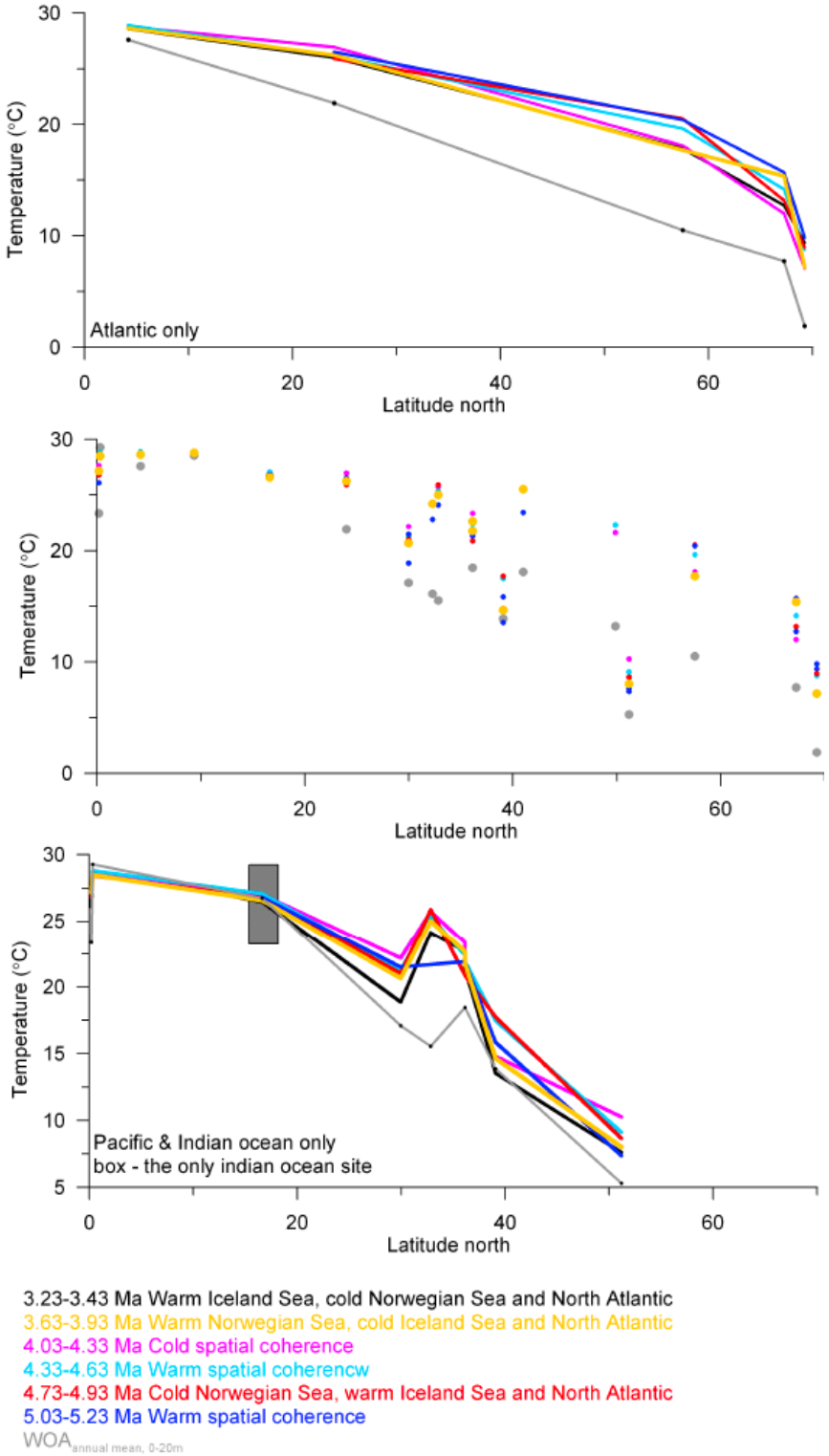

Figure S2. The identified Pliocene SST anomaly relations are shown together with planktic and benthic (1286 m water depth) Norwegian Sea/ODP Site 642B $\delta^{13}C$ anomalies, benthic $\delta^{13}C$ records from ODP Site 607 (red), 704 (blue) and 1264 (grey). The datasets $\delta^{13}C$ records from ODP Site 607, 704 and 1264 are used to calculate the percent North Atlantic Dep water (NADW), following (Bell et al., 2015). Grey, yellow and blue boxes along the x-axis represent spatial coherence, the Norwegian Sea SST anomaly being different from the North Atlantic and Iceland Sea SST anomalies, and the Iceland Sea SST anomaly being different from the North Atlantic and Norwegian Sea SST anomalies, respectively.

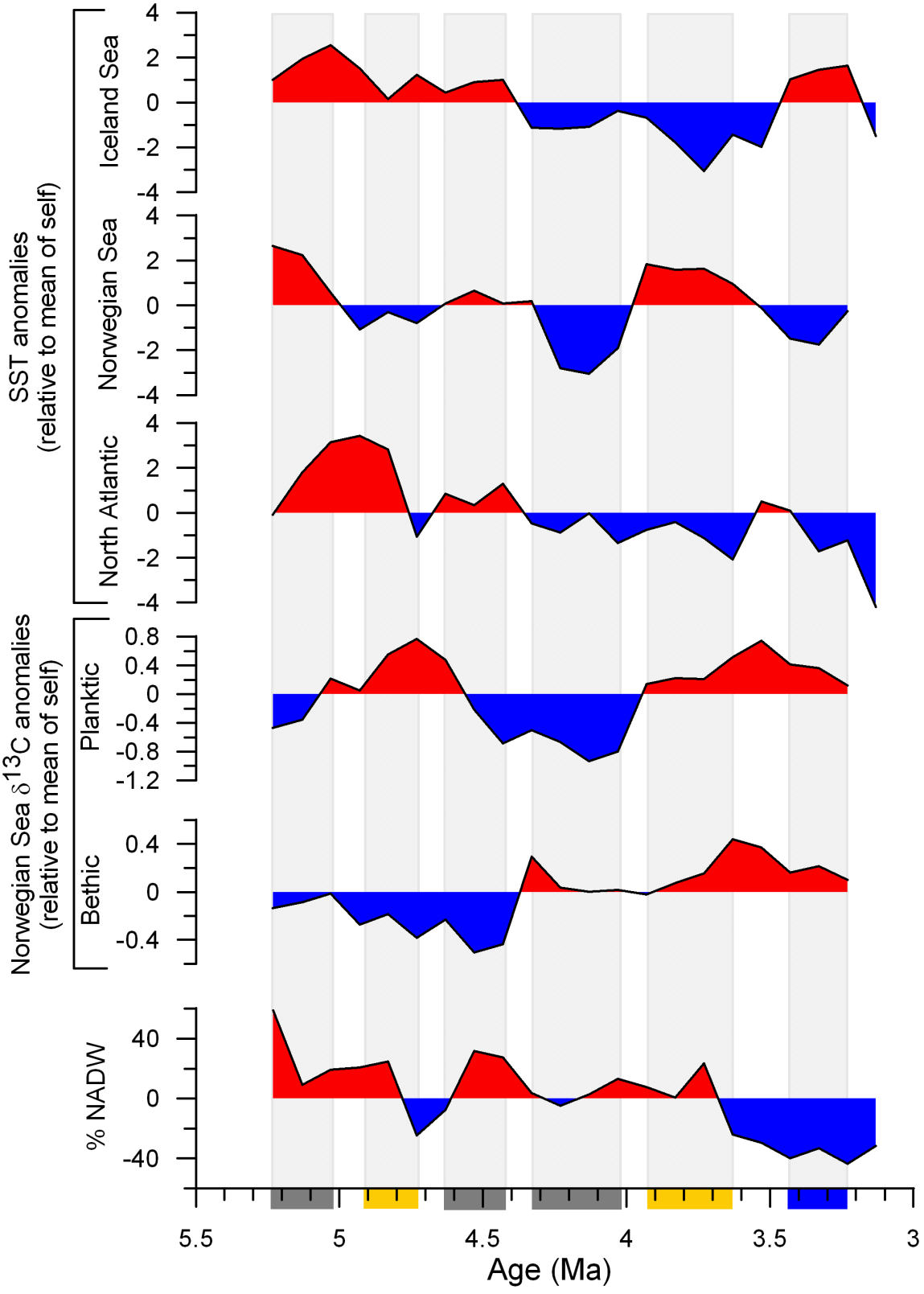

Figure S3. Globally distributed alkenone based SST records (data from sites in Table S1). In the left panel they are presented as anomaly relative to their own mean over the 5.23 to 3.13 Ma interval, based on the 100 ka resampled records. In the right panel absolute values for the 100 ka resampled datasets are shown; here the red fill shows when it was warmer at a specific site relative to $WOA_{annual\ mean\ 0\text{-}20m}$ (Locarini et al., 2018). Grey, yellow and blue boxes along the x-axis of the left panel represent times of spatial coherence, the Norwegian Sea SST anomaly being different from the North Atlantic and Iceland Sea SST anomalies, and the Iceland Sea SST anomaly being different from the North Atlantic and Norwegian Sea SST anomalies, respectively.

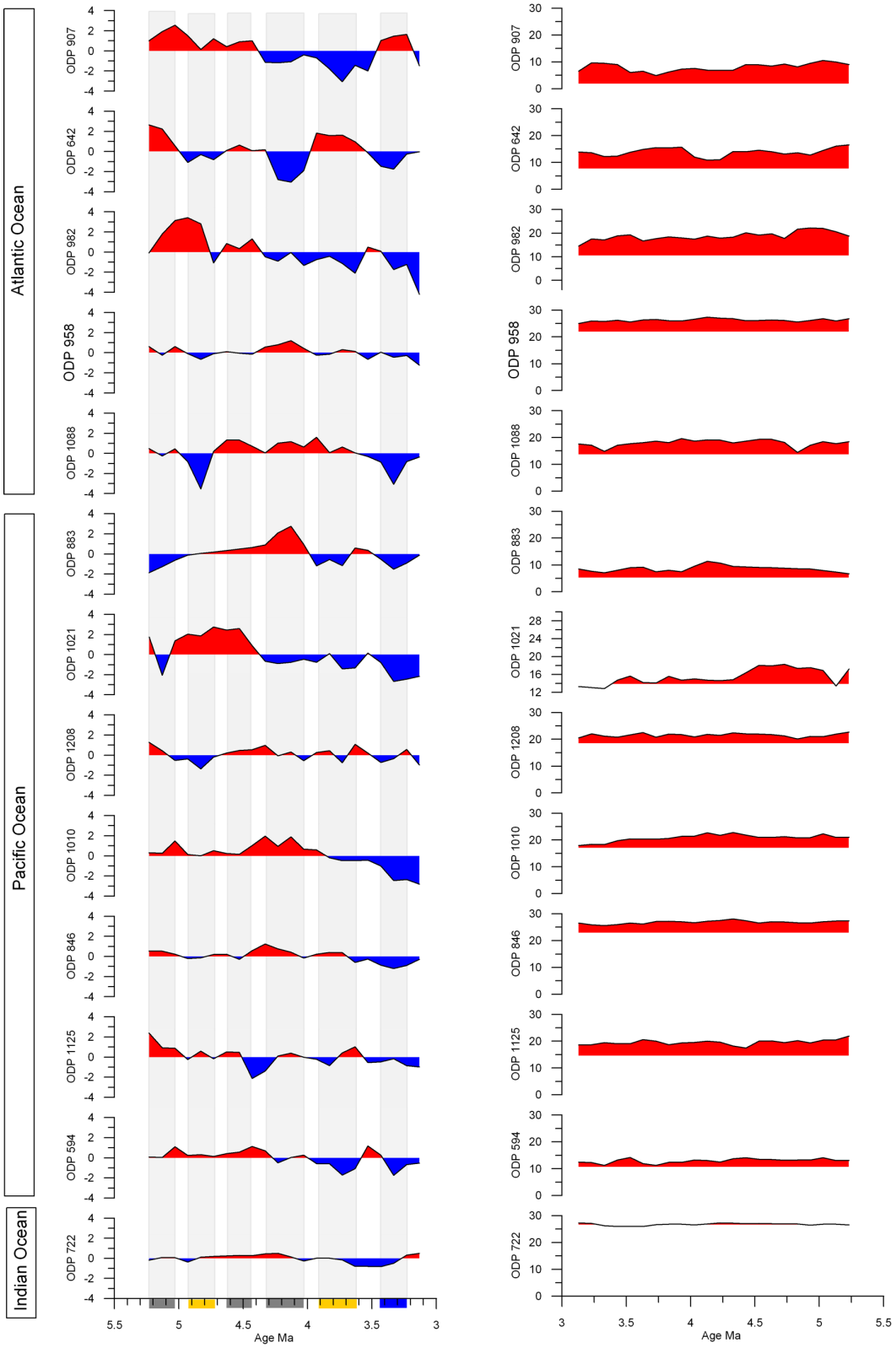

Figure S4. Meridional SST gradients. The upper panel shows data restricted to sites from the Atlantic Ocean and the lower panel show data restricted to sites from the Pacific and Indian Ocean using data from sites in Table S1. There is only one site with information from the Indian Ocean (marked with the box). The mid panel show all datapoints used for the upper and lower panel. The different coloured lines and dots represent time intervals where the different SST anomaly relations are identified (specified in the legend underneath). World Ocean Atlas data is from Locarini et al. (2018).

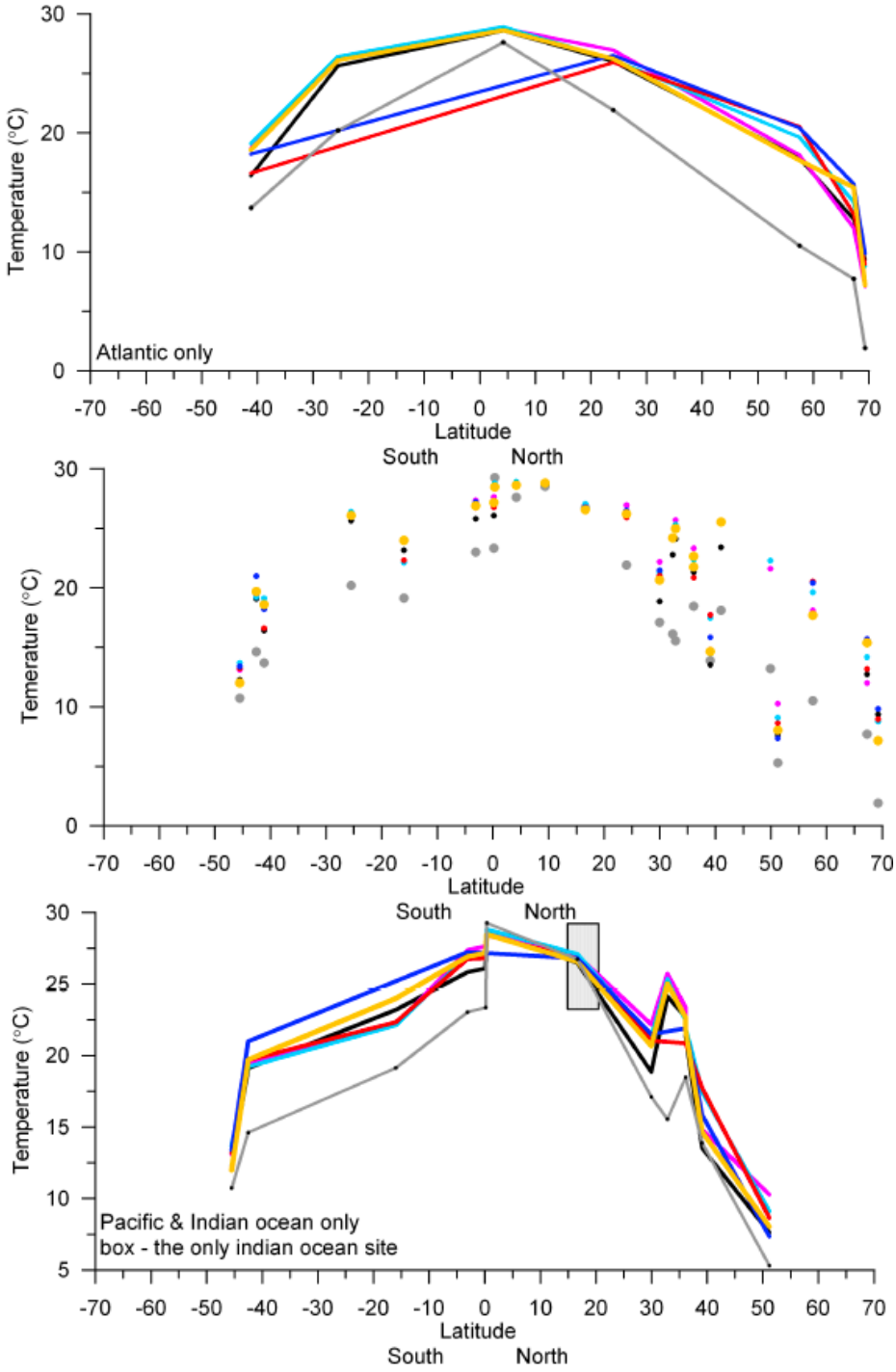

3.23-3.43 Ma Warm Iceland Sea, cold Norwegian Sea and North Atlantic
3.63-3.93 Ma Warm Norwegian Sea, cold Iceland Sea and North Atlantic
4.03-4.33 Ma Cold spatial coherence
4.33-4.63 Ma Warm spatial coherence
4.73-4.93 Ma Cold Norwegian Sea, warm Iceland Sea and North Atlantic
5.03-5.23 Ma Warm spatial coherence
WOA annual mean. 0-20m

Figure S5. The upper part of the figure shows the identified Pliocene SST anomaly relations, with the specific type of relation indicated by the grey, yellow and blue boxes at seen at the x-axis (with grey, yellow and blue boxes representing times of spatial coherence, the Norwegian Sea SST anomaly being different from the North Atlantic and Iceland Sea SST anomalies, and the Iceland Sea SST anomaly being different from the North Atlantic and Norwegian Sea SST anomalies, respectively). The lower part show the relative abundance of selected pollen types, as recorded from ODP Site 642 and interpreted to be representative of climate over Norway, closely connected to the Norwegian Sea SST development (Panitz et al., 2018).

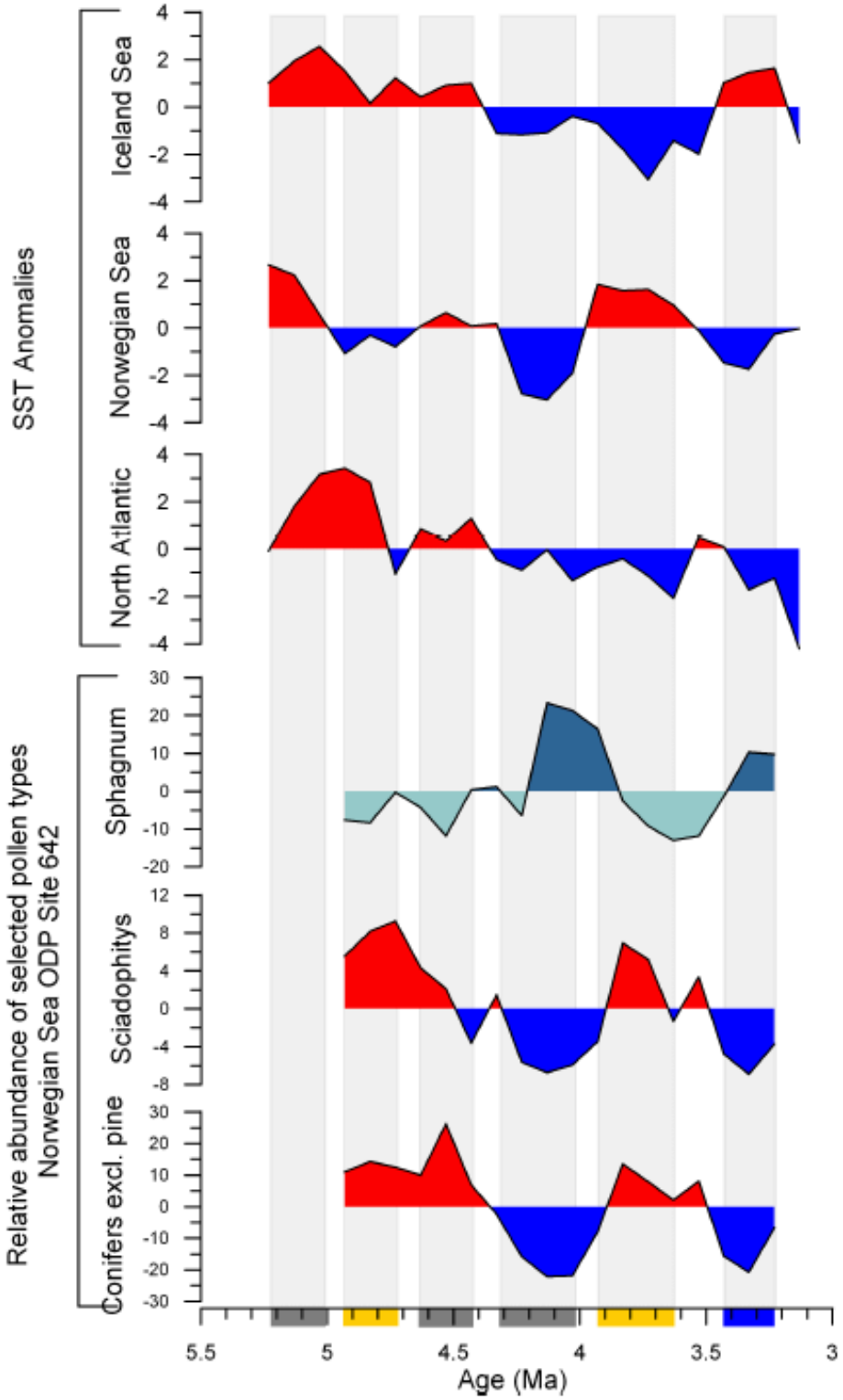

Figure S6. Map showing the location of sites used for the review of information feeding into Table 2 and shown in Fig. S1-S6. Black circles show locations with alkenone SST datasets. The red circles show the sites from where we have used benthic $\delta^{13}C$ datasets to indicate changes in ocean circulation. The base for the map is made with GeoMapApp (www.geomapapp.org) / CC BY / CC BY (Ryan et al., 2009)).

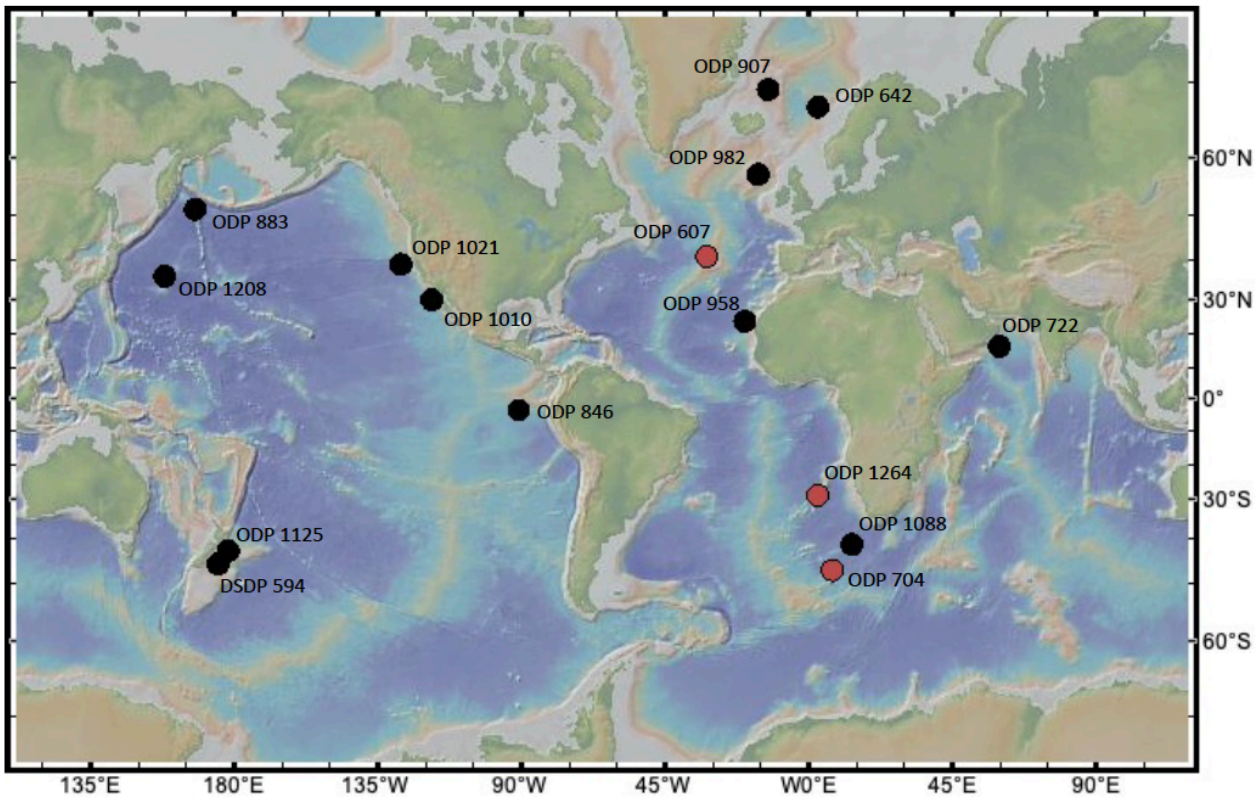

Table S1. Overview of sites and records used for Figures S1-S6, and hence feeding into Table 2. Original reference and reference to where we have collected the data is given.

Area	Site	Latitude	Longitude	Water depth (m)	Proxy used	Reference	Data source
>60°N Atlantic	ODP 907	69.24815	-12.69	1802	Alkenones	Herbert et al. (2016)	Herbert et al. (2016)
	ODP 642	67.255	2.928333	1281	Alkenones $\delta^{13}C$ Pollen	Bachem et al. (2017); Panitz et al. (2018); Risebrobakken et al. (2016)	https://doi.org/10.1594/PANGAEA.865205 https://doi.org/10.1594/PANGAEA.863867 Panitz et al. (2018)
30-60°N Atlantic	ODP 982	57.5167	-15.8667	1134	Alkenones	Herbert et al. (2016); Lawrence et al. (2009)	Herbert et al. (2016)
	DSDP 607	41.0012	-31.9573	3427	$\delta^{13}C$	Hodell and Venz-Curtis (2006)	Hodell and Venz-Curtis (2008)
30-60°N Pacific	ODP 1208	36.12716	158.20158	3346	Alkenones	Lariveire et al. (2012)	Herbert et al. (2016)
	ODP 1021	39.0875	-127.7832	4235	Alkenones	Lariveire et al. (2012)	Federov et al. (2013); Herbert et al. (2016)
	ODP 883	51.1983	167.7688	2396	Alkenones	Herbert et al. (2016)	Herbert et al. (2016)
30°S-30°N Atlantic	ODP 958	23.99895	-20.00083		Alkenones	Herbert and Schuffert (1998)	Federov et al. (2013)
	ODP 1264	-28.5325	2.8455	2505	$\delta^{13}C$	Bell et al. (2014)	ftp://ftp.ncdc.noaa.gov/pub/data/paleo/contributions_by_author/bell2014/bell2014-1264.txt
30°S-30°N Indian Ocean / Pacific	ODP 722	16.62187	59.79592	2028	Alkenones	Herbert et al. (2010); Huang et al. (2007)	Herbert et al. (2016)
	ODP 846	-3.094942	-90.81797	3296	Alkenones	Herbert et al. (2016); Lawrence et al. (2009); Liu and Herbert (2004)	Federov et al. (2013); Herbert et al. (2016)
	ODP 1010	29.96503	-118.1008	3464	Alkenones	Lariveire et al. (2012)	Federov et al. (2013); Herbert et al. (2016)
30-60°S Atlantic	ODP 1088	-41.13608	13.56285	2082	Alkenones	Herbert et al. (2016)	Herbert et al. (2016)
	ODP 704	-46.87975	7.420517	2532	$\delta^{13}C$	Hodell and Venz-Curtis (2006)	Hodell and Venz-Curtis (2008)
30-60°S Pacific	ODP 1125	-42.54967	178.1665	1365	Alkenones	Herbert et al. (2016)	Herbert et al. (2016)
	DSDP 594	-45.5235	174.948	1204	Alkenones	Herbert et al. (2016)	Herbert et al. (2016)

References

Bachem, P. E., Risebrobakken, B., De Schepper, S., and McClymont, E. L.: Highly variable Pliocene sea surface conditions in the Norwegian Sea, Clim. Past., 13, 1153-1168, https://doi.org/1110.5194/cp-1113-1153-2017, 2017.

Bell, D. B., Jung, S. J. A., Kroon, D., Lourens, L. J., and Hodell, D. A.: Local and regional trends in Plio-Pleistocene d18O records from benthic foraminifera, Geochem. Gephys. Geosyst., 15, 3304-3321, doi:3310.1002/2014GC005297, 2014.

Bell, D. B., Jung, S. J. A., Kroon, D., Hodell, D. A., Lourens, L. J., and Raymo, M. E.: Atlantic Deep-water Response to the Early Pliocene Shoaling of the Central American Seaway, Scientific Reports, 5, 12252, doi:12210.11038/srep12252, 2015.

Federov, A. V., Brierley, C., Lawrence, K. T., Liu, Z., Dekens, P. S., and Ravelo, A. C.: Patterns and mechanisms of early Pliocene warmth, Nature, 496, 43-52, 2013.

Herbert, T. D. and Schuffert, J. D.: Alkenone unsaturation estimates of late Miocene through late Pliocene sea surface temperature change, ODP site 958, Proc. ODP Sci. Res., 159T, 17-22, 1998.

Herbert, T. D., Cleavland Peterson, L., Lawrence, K. T., and Liu, Z.: Tropical ocean temperature over the past 3.5 million years, Science, 328, 1530-1534, 2010.

Herbert, T. D., Lawrence, K. T., Tzanova, A., Peterson, L. C., Caballero-Gill, R., and Kelly, C. S.: Late Miocene global cooling and the rise of modern ecosystems, Nature Geoscience, 9, 843-849, 2016.

Hodell, D. A. and Venz-Curtis, K. A.: Late Neogene history of deepwater ventilation in the Southern Ocean., Geochemistry, Geophysics, Geosystems, 7, Q09001, doi:09010.01029/02005GC001211, 2006.

Hodell, D. A. and Venz-Curtis, K. A.: Late Neogene Southern Ocean Carbon Isotope Data. [dataset], 2008.

Huang, Y., Clemens, S. C., Liu, W., Wang, Y., and Prell, W. L.: Large-scale hydrological change drove the late Miocene C4 plant expansion in the Himalayan foreland and Arabian Peninsula, Geology, 35, 531-534, https://doi.org/510.1130/G23666A.23661, 2007.

LaRiveire, J. P., Ravelo, A. C., Crimmins, A., Dekens, P. S., Ford, H. L., Lyle, M., and Wara, M. W.: Late Miocene decoupling of oceanic warmth and atmospheric cardon dioxide forcing, Nature, 486, 97-100, doi:110.1038/nature11200, 2012.

Lawrence, K. T., Herbert, T. D., Brown, C. W., Raymo, M., and Haywood, A. M.: High-amplitude variations in North Atlantic sea surface temperature during the early Pliocene warm period, Paleoceanography, 24, PA2218, doi:2210.1029/2008PA001669, 2009.

Liu, Z. and Herbert, T. D.: High-latitude influence on the eastern equatorial Pacific climate in the early Pleistocene epoch, Nature, 427, 720-723, 2004.
Locarini, R. A., Mishonov, A. V., Baranova, O. K., Boyer, T. P., Zweng, M. M., Garcia, H. E., Reagan, J. R., Seidov, D., Weathers, K., Paver, C. R., and Smolyar, I.: World Ocean Atlas 2018, Volume 1: Temperature, 52, 2018.
Paillard, D., Labeyrie, L., and Yiou, P.: Macintosh program performs time-series analysis, EOS, Trans. AGU, TI, 379, 1996.
Panitz, S., Salzmann, U., Risebrobakken, B., De Schepper, S., Pound, J. M., Haywood, A., Dolan, A. M., and Lunt, D.: Orbital, tectonic and oceanographic control of Pliocene climate and atmospheric circulation in Arctic Norway, Global Planetary Change, 161, 183-193, 2018.
Risebrobakken, B., Andersson, C., De Schepper, S., and McClymont, E. L.: Low-frequency Pliocene climate variability in the eastern Nordic Seas, Paleoceanography, 31, doi:10.1002/2015PA002918, 2016.
Ryan, W. B. F., Carbotte, S. M., Coplan, J., O'Hara, S., Melkonian, A., Arko, R., Weissel, R. A., Ferrini, V., Goodwillie, A., Nitsche, F., Bonczkowski, J., and Zemsky, R.: Global Multi-Resolution Topography (GMRT) synthesis data set, Geochem. Gephys. Geosyst., 10, QQ03014, doi:03010.01029/02008GC002332, 2009.